JOURNAL OF NEUROTRAUMA 34:213–219 (January 1, 2017)

DOI: 10.1089/neu.2015.4339

Early and Persistent Dendritic Hypertrophy in the Basolateral Amygdala following Experimental Diffuse Traumatic Brain Injury

Ann N. Hoffman,[1,5,6] Pooja R. Paode,[1] Hazel G. May,[2,3,7] J. Bryce Ortiz,[1] Salma Kemmou,[1] Jonathan Lifshitz,[1–4] Cheryl D. Conrad,[1] and Theresa Currier Thomas[2–4]

Abstract

In the pathophysiology of traumatic brain injury (TBI), the amygdala remains understudied, despite involvement in processing emotional and stressful stimuli associated with anxiety disorders, such as post-traumatic stress disorder (PTSD). Because the basolateral amygdala (BLA) integrates inputs from sensory and other limbic structures coordinating emotional learning and memory, injury-induced changes in circuitry may contribute to psychiatric sequelae of TBI. This study quantified temporal changes in dendritic complexity of BLA neurons after experimental diffuse TBI, modeled by midline fluid percussion injury. At post-injury days (PIDs) 1, 7, and 28, brain tissue from sham and brain-injured adult, male rats was processed for Golgi, glial fibrillary acidic protein (GFAP), or silver stain and analyzed to quantify BLA dendritic branch intersections, activated astrocytes, and regional neuropathology, respectively. Compared to sham, brain-injured rats at all PIDs showed enhanced dendritic branch intersections in both pyramidal and stellate BLA neuronal types, as evidenced by Sholl analysis. GFAP staining in the BLA was significantly increased at PID1 and 7 in comparison to sham. However, the BLA was relatively spared from neuropathology, demonstrated by an absence of argyrophilic accumulation over time, in contrast to other brain regions. These data suggest an early and persistent enhancement of dendritic complexity within the BLA after a single diffuse TBI. Increased dendritic complexity would alter information processing into and through the amygdala, contributing to emotional symptoms post-TBI, including PTSD.

Keywords: amygdala; comorbidity; plasticity; post-traumatic stress disorder; traumatic brain injury

Introduction

Traumatic brain injury (TBI) is a silent epidemic, which recently has been labeled the signature injury of current combat operations.[1] Long-term consequences of TBI include increased risk for neurological and psychiatric disorders, with anxiety disorders being particularly prevalent.[2–4] Increasing numbers of veterans exposed to both emotional and physical trauma have promoted interest in the comorbidity between TBI and post-traumatic stress disorder (PTSD), given that mild TBI is a significant predictor of PTSD subsequent to deployment.[5] Understanding how TBI impacts the neurocircuitry of emotional processing will help uncover mechanisms for future therapeutic targets.

The amygdala, a phylogenetically conserved limbic structure,[6] is involved in processing emotional and stressful stimuli[7,8] and is implicated in anxiety and PTSD.[9] Post-TBI, most cortical and subcortical regions show acute increases in glucose metabolism[10,11] and prolonged global oxidative metabolic depression.[12] In contrast, the amygdala demonstrates increased and persistent oxidative metabolic demands after experimental TBI using fluid percussion injury (FPI).[12] Pre-clinical models even show that FPI enhances fear learning and basolateral amygdala (BLA) excitatory processing with evidence of reduced GABAergic inhibition.[13,14] These studies suggest that the amygdala may respond to TBI differently than other brain regions.

TBI initiates pathomechanisms of structural plasticity throughout the brain in rats and humans,[15–17] where maladaptive outcomes can emerge from unguided repair and contribute to enduring symptoms and impairments in recovery of function.[18] The BLA receives rich inputs from sensory and limbic structures, demonstrates plasticity

[1]Department of Psychology, Arizona State University, Tempe, Arizona.
[2]Department of Child Health, University of Arizona College of Medicine-Phoenix, Phoenix, Arizona.
[3]Barrow Neurological Institute at Phoenix Children's Hospital, Phoenix, Arizona.
[4]Phoenix VA Healthcare System, Phoenix, Arizona.
[5]Department of Psychology, UCLA, Los Angeles, California.
[6]Brain Injury Research Center, Department of Neurosurgery, David Geffen School of Medicine at UCLA, Los Angeles, California.
[7]Department of Biology and Biochemistry, University of Bath, Bath, United Kingdom.

related to emotional learning,[19] and is sensitive to stress-induced structural changes that persist even after the stressors have ended.[20] Whether the BLA exhibits structural reorganization post-TBI remains unknown. Using the well-characterized FPI model, the aim of this study was to quantify the time course of alterations in dendritic arborization within the BLA after a single diffuse TBI, with respect to overall tissue pathology.

Methods

Fluid percussion brain injury

Adult male Sprague-Dawley rats (300–350 g; Harlan Laboratories Inc., Indianapolis, IN) were allowed access to food and water *ad libitum*, with all experiments and animal care conducted in accord with National Institutes of Health (NIH) and Institutional Animal Care and Use Committee–approved protocol. Rats were subjected to midline FPI, as previously described.[21,22] Rats were anesthetized (5% isoflurane), transferred to a stereotaxic frame (David Kopf Instruments, Tujunga, CA), maintained at 2% isoflurane, and 37°C body temperature monitored and maintained throughout the procedure. The skull was exposed and a 4.8-mm circular craniectomy was performed (centered on the sagittal suture midway between bregma and lambda) without disturbing the dura or superior sagittal sinus. A skull screw was secured into the right frontal bone. An injury hub was fabricated from the female portion of a Leur-Loc needle hub and affixed over the craniectomy using cyanoacrylate gel and methylmethacrylate (Hygenic Corp., Akron, OH). The incision was sutured at the anterior and posterior edges, and rats were then returned to a warmed holding cage until ambulation returned.

Approximately 60–90 min after the conclusion of the surgical procedure, animals were reanesthetized (5% isoflurane). The female end of the injury hub assembly was filled with physiological saline and attached to the male end of the fluid percussion device (Custom Design and Fabrication; Virginia Commonwealth University, Richmond, VA). Upon the return of the pedal withdrawal reflex, an injury of moderate severity (1.8–2.0 atmospheres) was administered by releasing the pendulum onto the fluid-filled piston. Sham animals were connected to the FPI device, but the pendulum was not released. Afterward, the injury hub assembly was removed *en bloc*, the craniotomy was inspected, and the incision was sutured. Animals were monitored for the fencing response upon impact,[21] changes in respiration, and the return of the righting reflex. A moderate-severity brain injury was determined by recovery of a righting reflex in 5–10 min. Sham-injured animals recovered within 15 sec.

Golgi stain

At post-injury day (PID) 1, 7, and 28, sham and brain-injured rats ($n = 4$/group) were overdosed with sodium pentabarbitol (200 mg/kg, intraperitoneally), decapitated, and the brain rapidly removed. At least 1 sham-operated animal was euthanized at each PID time point. The brain was processed for Golgi staining according to the manufacturer's instructions for the FD Rapid GolgiStain™ Kit (FD NeuroTechnologies, Inc., Columbia, MD). Brains were sectioned (200 μm) at –22°C on a cryostat and mounted on slides. Neurons were selected using the following criteria: 1) cell body and

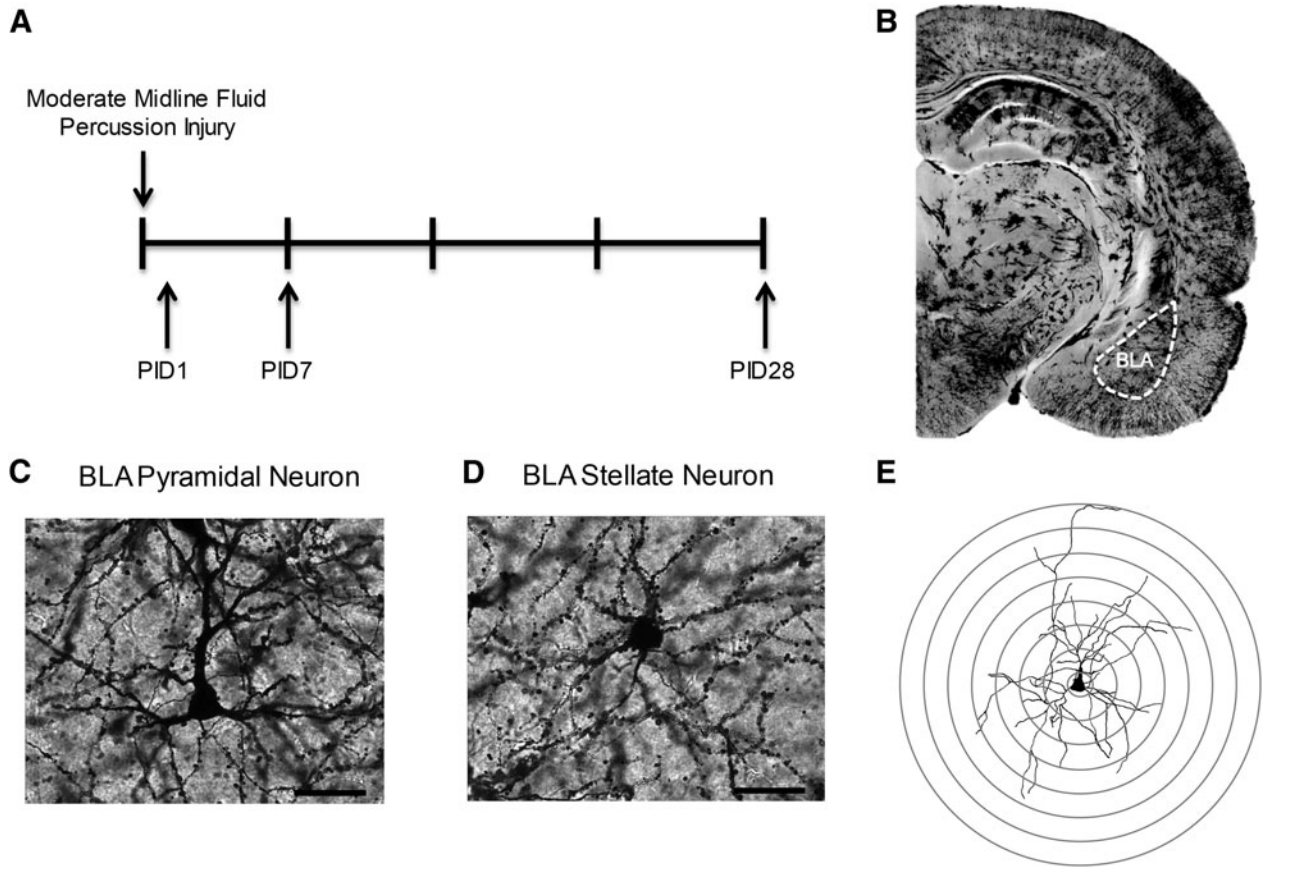

FIG. 1. Experimental methods. (**A**) Experimental timeline; brains were processed and bilateral BLA were analyzed for Golgi and silver stains at post-injury day (PID) 1, 7, and 28. (**B**) Golgi stain coronal hemisection depicting BLA. (**C** and **D**) Representative impregnated (C) pyramidal and (D) spiny stellate BLA neurons. Images are at 40×; Scale bar = 50 μm. (**E**) Example of reconstructed neuron with overlaid Sholl rings. BLA, basolateral amygdala.

dendrites were fully impregnated and untruncated; 2) cell was relatively isolated; 3) within the BLA, and 4) identified as stellate or pyramidal subtype. Because of the low number of fully stained cells, all BLA and pyramidal and stellate neurons that matched these criteria were included in the quantification and analysis. Stellate neurons expressed round somas, with spiny dendrites radiating outward in all directions (Fig. 1). Pyramidal neurons expressed triangular-like somas with a prominent apical dendrite that arose from the superficial pole of the cell body and several thinner basal dendrites on the opposite side (Fig. 1). Neurons were traced at 320× using a camera lucida drawing tube attached to an Olympus BX51 microscope (Olympus, Tokyo, Japan) and quantified by Sholl analysis.[25,26] Dendritic intersections were quantified at equidistant concentric circles in 20-μm increments from the soma. Number of cells/rat ranged from 4 to 9 for stellate neurons and 4 to 8 for pyramidal neurons. A Sholl analysis comparing sham animals confirmed there was no significant difference between animals, and the shams were combined into one sham cohort. Data were averaged across same cell types within each animal and analyzed across animals for each experimental group and cell type.

Silver stain

Argyrophilic reaction product was analyzed in the BLA of a separate cohort of sham ($n=3$, one at each time point) or FPI rats at PID1, 7, and 28 ($n=3$/time point). As described by Lifshitz and Lisembee,[27] rats were prepared using NeuroScience Associates Inc. (Knoxville, TN) instructions. Brains were shipped to NeuroScience Associates to be embedded into a single gelatin block (Multiblock® Technology; NeuroScience Associates), cryosectioned, mounted, and stained with the de Olmos aminocupric silver staining technique, and counterstained with Neutral Red, in accord to proprietary protocols.

Stained sections were analyzed in our laboratory.[27] Photomicrographs of silver stained BLA from both hemispheres were taken using a Zeiss microscope (Imager A2; Carl Zeiss, Jena, Germany) in bright-field mode with a digital camera. Densitometric quantitative analysis was performed at 20× using ImageJ software (1.48v; NIH, Bethesda, MD). Grayscale digital images were digitally thresholded to separate positive stained pixels from unstained pixels, then segmented into black and white pixels, indicative of positive and negative staining, respectively. The percentage of argyrophilic (black) stained pixels was calculated for each image using the following formula: *[count/total area measured]×100=percentage area stained black*; where *count* is the total number of black pixels. Eight images were analyzed per animal, with the percentage of black pixels averaged to a single value (per animal) and used in data analysis.

Glial fibrillary acidic protein

At PID1, 7, and 28, sham and brain-injured rats were overdosed with sodium pentabarbitol and transcardially perfused with phosphate-buffered saline (PBS) and 4% paraformaldehyde (n=4–6/time point; at least 1 sham at each time point). Brains were immersed in serial sucrose dilutions (15%, 30%) and cryosectioned (20 μm). Sections were washed 3× with 1XPBS, blocked with 4% (v/v) normal horse serum in PBS for 1 h, incubated in the primary antibody (rabbit anti-GFAP, 1:1000; catalog no.: Z0334; Dako, Carpinteria, CA) overnight at room temperature, rinsed in 1XPBS, incubated for 1 h at room temperature with the secondary antibody (biotinylated horse anti-rabbit, 1:250; catalog no.: BA-1100; Vector Laboratories, Burlingame, CA), washed, blocked with 0.3% hydrogen peroxide, incubated with avadin/biotin complex (4°C, 20 min), washed, and incubated with 3,3′-diaminobenzidine (10 min). Sections were dehydrated with ethanol, cleared in CitriSolv, and cover-slipped using distyrene plasticizer xylene. Densitometric quantitative analysis was performed identical to silver stain.

Statistical analysis

Statistical analyses were conducted using SPSS software (v.22; IBM Corp., Armonk, NY) using a Macintosh computer (OSX 10.9.5). Dendritic complexity was analyzed by a mixed-factor analysis of variance (ANOVA) for treatment condition (sham, PID1, PID7, and PID28) across the distances from the soma. GFAP and silver stain was analyzed by one-way ANOVA for time post-injury. When statistical significance was reached at $p<0.05$, least significant differences (LSD) post-hoc analyses were performed and described where indicated.

Results

Diffuse traumatic brain injury increased basolateral amygdala dendritic branch intersections

FPI resulted in a significant change in dendritic branch intersections in BLA pyramidal neurons (Fig. 2). A mixed-factors ANOVA between time post-injury and across distance from the soma (20-μm increments from 20 to 400 μm) revealed a significant PID × distance interaction ($F_{(57,209)}=2.565$; $p<0.001$) for the number of dendritic branch intersections. Specifically, LSD post-hoc analyses revealed an increased number of branch intersections in BLA pyramidal neurons proximal to the soma within 1 day post-injury (PID1 compared to sham, $p<0.05$; 40 and 80 μm from soma), which persisted at PID7 (compared to sham, $p<0.05$; 40 and 80 μm from soma), and PID28 (compared to sham, $p<0.05$; 40 μm from soma). Further, BLA pyramidal neurons showed increased numbers of intersections in distal dendrites at PID28 (compared to sham, $p<0.05$; 380–400 μm from soma). These data indicate an injury-induced

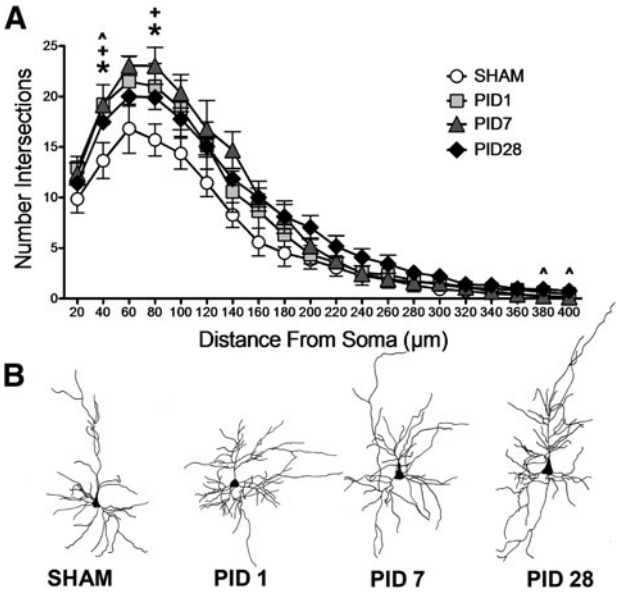

FIG. 2. Dendritic arborization in basolateral amygdala (BLA) pyramidal after fluid percussion injury (FPI). (**A**) FPI increased BLA pyramidal neuron dendritic complexity proximal to the soma by post-injury day (PID) 1, and dendritic hypertrophy persisted on PID7 and 28. At PID28, BLA distal dendrites showed additional hypertrophy. Data are represented as mean ± standard error of the mean; $p<0.05$ for all comparisons. *PID1 versus SHAM; $^{+}$PID7 versus SHAM; $^{\wedge}$PID28 versus SHAM. (**B**) Representative reconstructions of BLA pyramidal neurons for each post-injury time point. Note: pyramidal neuron orientation adjusted to depict apical dendrites pointing upward.

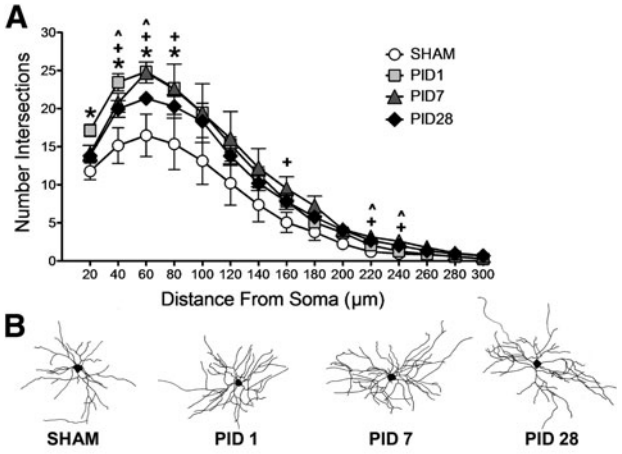

FIG. 3. Dendritic arborization in basolateral amygdala (BLA) stellate neurons after fluid percussion injury (FPI). (**A**) FPI increased BLA stellate neuron dendritic complexity proximal to the soma by post-injury day (PID) 1, and dendritic hypertrophy persisted on PID7 and 28. At PID7 and 28, BLA distal dendrites showed additional hypertrophy. $p < 0.05$ for all comparisons. *PID1 versus SHAM; $^{+}$PID7 versus SHAM; $^{\wedge}$PID28 versus SHAM. (**B**) Representative reconstructions of BLA stellate neurons for each post-injury time point.

enhancement in dendritic complexity of pyramidal neurons near the soma that occurs acutely and endures through PID28, at which time additional restructuring of distal dendrites occurs.

Similar patterns were found for BLA stellate neurons. A mixed-factors ANOVA between time post-injury and across distance from soma (every 20 μm from 20 to 300 μm) revealed a significant main effect of PID ($F_{(3,11)} = 5.581$; $p = 0.014$) and a significant PID $\times$ distance interaction ($F_{(42,154)} = 3.287$; $p < 0.001$). Specifically, LSD post-hoc analyses revealed that FPI increased the number of intersections proximal to the soma (20–80 μm) by PID1 compared to sham ($p < 0.05$), and the increased number of intersections persisted at PID7 (compared to sham, $p < 0.05$; 40–80 μm) and PID28 (compared to sham, $p < 0.05$; 40–60 μm). At later time points, injured BLA distal dendrites had increased levels of dendritic branching (PID7 compared to sham, $p < 0.05$; 160 and 220–240 μm; PID28 compared to sham, $p < 0.05$; 220–240 μm from soma; Fig. 3). Further, complexity between PIDs in BLA stellate neurons was robust, with the greatest amount of intersections proximal to the soma at 1 day post-injury relative to the subsequent time points (PID1 compared to PID7 at 20 and 60, $p < 0.05$; and PID1 compared to PID28 at 20, 40, and 60 μm, $p < 0.05$). These data indicate an injury-induced enhancement in dendritic complexity in both pyramidal and stellate neurons in the BLA near the soma that occurs acutely and endures chronically, when additional restructuring of distal dendrites occurs.

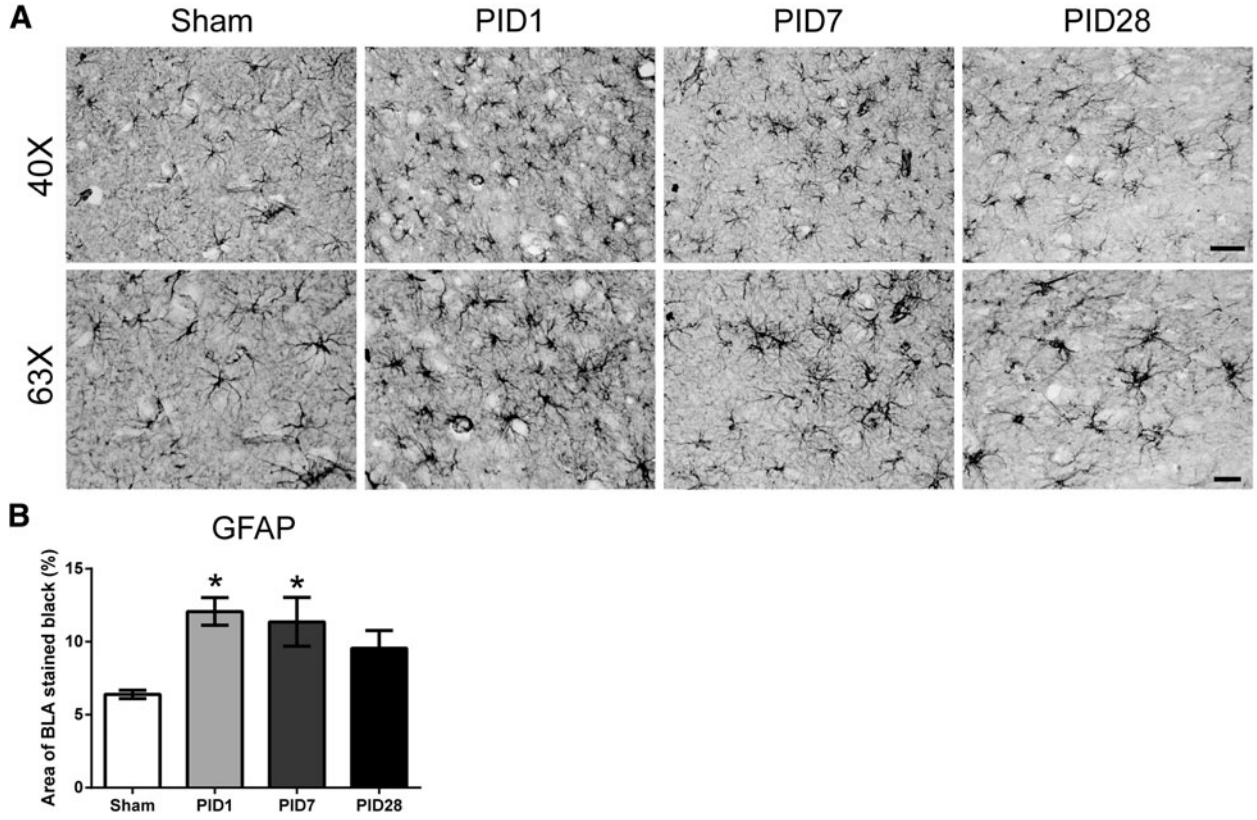

FIG. 4. Diffuse traumatic brain injury transiently increases activated astrocytes in the BLA. (**A**) GFAP staining increases and astrocyte morphology changes indicate activated astrocytes. Representative images are presented at 40$\times$(scale bar = 40 μm) and 63$\times$(scale bar = 20 μm). (**B**) Quantification of GFAP staining shows a significant difference between PID1 and PID7 compared to sham (sham = 4; PID1 = 6; PID7 = 4, and PID28 = 4; data are represented as mean $\pm$ standard error of the mean). BLA, basolateral amygdala; GFAP, glial fibrillary acidic protein; PID, post-injury day.

Activated astrocytes in the absence of overt neuropathology in the basolateral amygdala after diffuse traumatic brain injury

Astrocyte morphology at PID1 and 7 showed intense GFAP staining and cellular hypertrophy, indicative of activated astrocytes. GFAP immunoreactivity significantly increased as a function of time post-injury in the BLA ($F_{(3,14)} = 5.142$; $p = 0.013$; Fig. 4). Post-hoc analysis revealed that the percent area of BLA stained for GFAP was increased by 89% at PID1 and 78% at PID7 in comparison to sham ($p < 0.05$). At PID28, there was no detectable difference.

Whereas silver accumulation after diffuse TBI has indicated neuropathology in specific brain areas over time, for example, primary somatosensory barrel cortex,[27] a relative absence of staining was observed in the BLA of the same animals. On average, the percent of argyrophilic staining in sham animals was $3.6 \pm 1.5\%$, with no change over time post-injury ($F_{(3,8)} = 3.03$; $p = 0.09$; Fig. 5), indicating that a single TBI did not cause prominent neuropathology in the BLA.

Discussion

We present evidence for structural plasticity within the BLA after diffuse TBI, which has not previously been described. Data show early (within a day) and persistent enhancement in dendritic branch complexity in two predominate cell types within the BLA after a single diffuse TBI. The Sholl analysis indicates that BLA neurons exhibit increased dendritic intersections proximal to the soma at PID1, 7, and 28. At later time points, BLA neurons have more dendritic intersections at distal dendrites (PID28 for pyramidal and PID7 and PID28 for stellate cells). GFAP immunoreactivity increased at PID1 and 7, supporting a role for activated astrocytes in the post-traumatic sequelae in the BLA. Silver stain further revealed that the BLA is spared of overt neuropathology, in contrast to other diffuse-injured brain regions.[27] Together, these data indicate that diffuse TBI causes early and persistent dendritic hypertrophy in the BLA in the absence of neuropathology, possibly supported by activated astrocytes.

Few studies have investigated alterations in dendritic structural plasticity after models of TBI in vulnerable brain regions. In the cortex, lateral FPI-induced enhanced dendritic branching in regions remote from the injury site in immature rats.[28] At 1 month, focal TBI by controlled cortical impact (CCI) decreased dendritic length and branch points in pyramidal neurons in the hippocampal CA1 of rats injured at PID17, but not rats injured at PID7.[29] In contrast, moderate severity CCI led to dendritic atrophy in hippocampal dentate gyrus neurons in adult rats that may correspond with impaired recovery of function post-injury.[18] Further, our lab has shown that 1 week after midline FPI, thalamic neurons show dendritic retraction that recover to sham levels by PID28.[30] Importantly, these reductions observed in thalamic circuitry were discovered using the same tissue as our current BLA data, demonstrating region-specific effects of TBI. Together, these findings implicate widespread and dynamic region-specific alterations in structural plasticity as measured by changes in dendritic branching after brain injury that may influence onset of neurological sequelae post-TBI.

TBI could be classified as an inherent physical stressor, leading to activation of the sympathetic nervous system and hypothalamic-pituitary-adrenal (HPA) axis.[31,32] Stress and glucocorticoids involve amygdala engagement,[31] which may be a mechanism underlying the observed FPI-induced BLA structural enhancement. Repeated immobilization stress affects structural plasticity within the limbic system, including dendritic hypertrophy in the BLA that

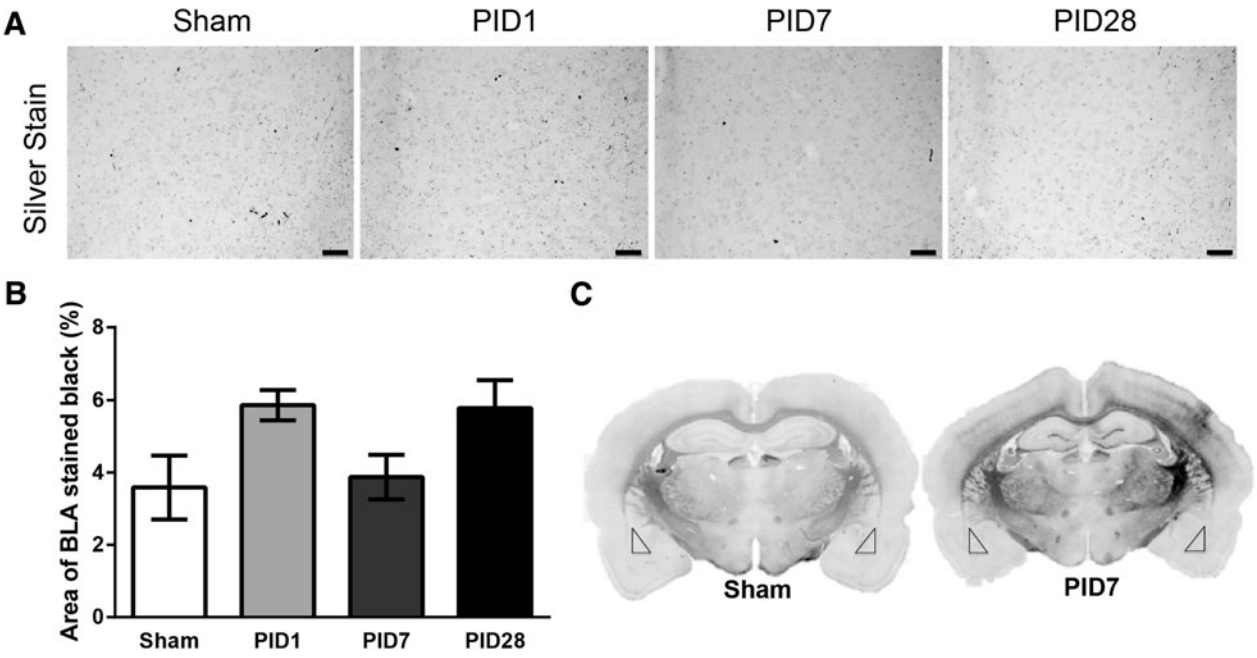

FIG. 5. Lack of overt neuropathology in the BLA after diffuse traumatic brain injury. (**A**) Images of the BLA in de Olmos silver stained sections in sham, PID1, PID7, and PID28 animals ($20\times$ magnification; scale bar $= 50\,\mu$m). (**B**) Quantification of silver staining indicates no detectable differences in neuropathology between sham and injured animals over time post-injury ($n = 4$/PID; all bar graphs represent the mean ± standard error of the mean). (**C**) Montages of silver stained coronal sections from a representative sham and PID7 animal. Bilateral neuropathology in the cortex, hippocampus, thalamus, corpus callosum, and internal capsule by PID7 can be visually detected in comparison to the same region in the sham control. At 7 days post-injury, staining in the BLA (triangles) is similar to sham. BLA, basolateral amygdala; PID, post-injury day.

persists for at least 21 days after chronic stressor termination, that corresponds with increased anxiety-like behavior.[20,33] In clinical TBI cases, HPA axis activation may be augmented above the stress response from physical stress independent of brain injury (i.e., peripheral orthopedic injury).[34,35] In experimental TBI, FPI and sham surgery both caused a peak HPA response; however, only FPI enhanced corticotrophin releasing hormone (CRH) messenger RNA (mRNA) expression in the hypothalamus,[36] which was also demonstrated by CRH mRNA in the amygdala.[37] Combined with the current results, the amygdala proves to be an exquisitely sensitive structure to glucocorticoids from robust and even mild stressors (exogenous or endogenous), and demonstrates resistance to recovery, providing a potential mechanism that could influence long-term functional outcome post-TBI and warrants future research to test causality.

Dendritic hypertrophy of pyramidal and stellate neurons may be indicative of increased communication between extra-amygdala structures and within the amygdala, respectively. Pyramidal neurons within the BLA are excitatory projection neurons that communicate with other amygdala subregions and long-range projection sites distributed throughout the brain, including cortical and other limbic structures.[38,39] Nonpyramidal stellate neurons are thought to be local circuit neurons,[38] with the stellate neurons included in the current study being spine-dense and of similar soma size, representing excitatory glutamatergic neurons.[40,41] Given that we observed extended dendritic branching in both cell types at distal portions of the cell at late time points, this suggests that long-term changes at distal dendrites reflects extended dendritic branching late post-injury that may influence long-term enhanced excitability in the BLA, perhaps by increased local dendritic signaling by greater degrees of action potential back-propagation at these sites.[42] Further, the observed effects were consistent across groups with relatively small sample sizes ($n = 4$/group), with relative changes across the cell that emphasize the power of the effect within the BLA suggesting amygdala sensitivity to TBI.

The observed structural changes after a single diffuse TBI occur in the absence of overt neuropathology. Previous experiments demonstrated no loss of neurons in the BLA at PID7 or 30 after lateral FPI in the mouse.[43] Another study failed to detect degenerating neurons in the amygdala by Fluoro-Jade staining in the subacute phase (PID1, 2, and 7) post-FPI or weight drop experimental TBI.[44] However, the increase of GFAP immunoreactivity in the absence of a destructive lesion or neuropathology can indicate astrocytic support of neuritic extension and axon regeneration through expression of a subset of surface molecules and neurotrophic factors.[45] It remains to be shown whether growth-promoting molecules, such as growth-associated protein 43 and brain-derived neurotrophic factor, contribute to dendritic hypertrophy within the BLA. These data support injury-induced circuit reorganization within the amygdala, below detection level of advanced clinical imaging, which can contribute to persisting emotional deficits.

The amygdala is a key anatomical locus implicated in comorbid mood and anxiety disorders, such as PTSD. Although we did not directly investigate functional outcome, the current results for excitatory neuronal subtypes provide a framework for future studies to investigate the early and long-term involvement of the amygdala in neurological consequences of TBI. Our data may implicate enhanced excitatory processing within, and perhaps beyond, the amygdala post-TBI,[14] and one may also speculate reduced inhibition.[13] Moreover, our results on amygdala structural changes after diffuse TBI through midline FPI add to the growing literature on the effects of TBI on anxiety-like and fear behavior in models of blast TBI[46–48] and weight drop.[49] Important to note, the BLA consists of multiple subpopulations of pyramidal neurons, which may play differential functional roles in fear expression and inhibition.[50,51] However, whether TBI would affect dendritic branching differently across these distinct functional subtypes of glutamatergic neurons remains unknown and is an objective for future research. Regardless, amygdala emotional circuits are reforming acutely and chronically after diffuse TBI, which can elicit, or at least contribute to, the spectrum of neurological symptoms associated with clinical TBI. TBI-induced hyperconnectivity in glutamateric neurons of the amygdala could impact emotional learning and anxiety that is observed with the increasing incidences of comorbid TBI and PTSD, an interaction that warrants continued investigation.

Acknowledgments

The authors thank Elizabeth Peck and Amanda Lisembee. Supported by the Arizona Biomedical Research Commission through the Arizona Department of Health Services (ADHS14-00003606), National Institute of Neurological Disorders and Stroke of the National Institutes of Health (R01 NS-065052), and Phoenix Children's Hospital Mission Support Funds.

Author Disclosure Statement

No competing financial interests exist.

References

1. Snell, F.I., and Halter, M.J. (2010). A signature wound of war: mild traumatic brain injury. J. Psychosoc. Nurs. Ment. Health Serv. 48, 22–28.
2. Rao, V., and Lyketsos, C. (2000). Neuropsychiatric sequelae of traumatic brain injury. Psychosomatics 41, 95–103.
3. Moore, E.L., Terryberry-Spohr, L., and Hope, D.A. (2006). Mild traumatic brain injury and anxiety sequelae: a review of the literature. Brain Inj. 20, 117–132.
4. Vaishnavi, S., Rao, V., and Fann, J.R. (2009). Neuropsychiatric problems after traumatic brain injury: unraveling the silent epidemic. Psychosomatics 50, 198–205.
5. Yurgil, K.A., Barkauskas, D.A., Vasterling, J.J., Nievergelt, C.M., Larson, G.E., Schork, N.J., Litz, B.T., Nash, W.P., and Baker, D.G.; Marine Resiliency Study Team. (2014). Association between traumatic brain injury and risk of posttraumatic stress disorder in active-duty Marines. JAMA Psychiatry 71, 149–157.
6. Moreno, N., and Gonzalez, A. (2007). Evolution of the amygdaloid complex in vertebrates, with special reference to the anamnio-amniotic transition. J. Anat. 211, 151–163.
7. LeDoux, J. (2003). The emotional brain, fear, and the amygdala. Cell. Mol. Neurobiol. 23, 727–738.
8. Fendt, M., and Fanselow, M.S. (1999). The neuroanatomical and neurochemical basis of conditioned fear. Neurosci. Biobehav. Rev. 23, 743–760.
9. Shin, L.M., Rauch, S.L., and Pitman, R.K. (2006). Amygdala, medial prefrontal cortex, and hippocampal function in PTSD. Ann. N. Y. Acad. Sci. 1071, 67–79.
10. Kawamata, T., Katayama, Y., Hovda, D.A., Yoshino, A., and Becker, D.P. (1992). Administration of excitatory amino acid antagonists via microdialysis attenuates the increase in glucose utilization seen following concussive brain injury. J. Cereb. Blood Flow Metab. 12, 12–24.
11. Yoshino, A., Hovda, D.A., Kawamata, T., Katayama, Y., and Becker, D.P. (1991). Dynamic changes in local cerebral glucose utilization following cerebral conclusion in rats: evidence of a hyper- and subsequent hypometabolic state. Brain Res. 561, 106–119.
12. Hovda, D.A., Yoshino, A., Kawamata, T., Katayama, Y., and Becker, D.P. (1991). Diffuse prolonged depression of cerebral oxidative metabolism following concussive brain injury in the rat: a cytochrome oxidase histochemistry study. Brain Res. 567, 1–10.
13. Almeida-Suhett, C.P., Prager, E.M., Pidoplichko, V., Figueiredo, T.H., Marini, A.M., Li, Z., Eiden, L.E., and Braga, M.F. (2014). Reduced GABAergic inhibition in the basolateral amygdala and the development

of anxiety-like behaviors after mild traumatic brain injury. PLoS One 9, e102627.
14. Reger, M.L., Poulos, A.M., Buen, F., Giza, C.C., Hovda, D.A., and Fanselow, M.S. (2012). Concussive brain injury enhances fear learning and excitatory processes in the amygdala. Biol. Psychiatry 71, 335–343.
15. Kou, Z., and Iraji, A. (2014). Imaging brain plasticity after trauma. Neural Regen. Res. 9, 693–700.
16. Bramlett, H.M., and Dietrich, W.D. (2002). Quantitative structural changes in white and gray matter 1 year following traumatic brain injury in rats. Acta Neuropathol. 103, 607–614.
17. Kim, J., Avants, B., Patel, S., Whyte, J., Coslett, B.H., Pluta, J., Detre, J.A., and Gee, J.C. (2008). Structural consequences of diffuse traumatic brain injury: a large deformation tensor-based morphometry study. Neuroimage 39, 1014–1026.
18. Gao, X., Deng, P., Xu, Z.C., and Chen, J. (2011). Moderate traumatic brain injury causes acute dendritic and synaptic degeneration in the hippocampal dentate gyrus. PLoS One 6, e24566.
19. Fanselow, M.S., and LeDoux, J.E. (1999). Why we think plasticity underlying Pavlovian fear conditioning occurs in the basolateral amygdala. Neuron 23, 229–232.
20. Vyas, A., Pillai, A.G., and Chattarji, S. (2004). Recovery after chronic stress fails to reverse amygdaloid neuronal hypertrophy and enhanced anxiety-like behavior. Neuroscience 128, 667–673.
21. Hosseini, A.H., and Lifshitz, J. (2009). Brain injury forces of moderate magnitude elicit the fencing response. Med. Sci. Sports Exerc. 41, 1687–1697.
22. Thomas, T.C., Hinzman, J.M., Gerhardt, G.A., and Lifshitz, J. (2012). Hypersensitive glutamate signaling correlates with the development of late-onset behavioral morbidity in diffuse brain-injured circuitry. J. Neurotrauma 29, 187–200.
23. Mitra, R., Jadhav, S., McEwen, B.S., Vyas, A., and Chattarji, S. (2005). Stress duration modulates the spatiotemporal patterns of spine formation in the basolateral amygdala. Proc. Natl. Acad. Sci. U. S. A. 102, 9371–9376.
24. Ranft, A., Kurz, J., Deuringer, M., Haseneder, R., Dodt, H.U., Zieglgansberger, W., Kochs, E., Eder, M., and Hapfelmeier, G. (2004). Isoflurane modulates glutamatergic and GABAergic neurotransmission in the amygdala. Eur. J. Neurosci. 20, 1276–1280.
25. Taylor, S.B., Anglin, J.M., Paode, P.R., Riggert, A.G., Olive, M.F., and Conrad, C.D. (2014). Chronic stress may facilitate the recruitment of habit- and addiction-related neurocircuitries through neuronal restructuring of the striatum. Neuroscience 280C, 231–242.
26. Uylings, H.B., and van Pelt, J. (2002). Measures for quantifying dendritic arborizations. Network 13, 397–414.
27. Lifshitz, J., and Lisembee, A.M. (2012). Neurodegeneration in the somatosensory cortex after experimental diffuse brain injury. Brain Struct. Funct. 217, 49–61.
28. Ip, E.Y., Giza, C.C., Griesbach, G.S., and Hovda, D.A. (2002). Effects of enriched environment and fluid percussion injury on dendritic arborization within the cerebral cortex of the developing rat. J. Neurotrauma 19, 573–585.
29. Casella, E.M., Thomas, T.C., Vanino, D.L., Fellows-Mayle, W., Lifshitz, J., Card, J.P., and Adelson, P.D. (2014). Traumatic brain injury alters long-term hippocampal neuron morphology in juvenile, but not immature, rats. Childs. Nerv. Syst. 30, 1333–1342.
30. Rumney, B.M., Khodadad, A., Adelson, P.D., Lifshitz, J., and Thomas, T.C. (2014). Morpholgoical reorganization of thalamic neurons after diffuse TBI may underlie attenuated immediate early gene activation, in: *The 32nd Annual National Neurotrauma Symposium*. San Francisco, CA: Mary Ann Liebert, Inc.
31. Herman, J.P., Figueiredo, H., Mueller, N.K., Ulrich-Lai, Y., Ostrander, M.M., Choi, D.C., and Cullinan, W.E. (2003). Central mechanisms of stress integration: hierarchical circuitry controlling hypothalamo-pituitary-adrenocortical responsiveness. Front. Neuroendocrinol. 24, 151–180.
32. Selye, H. (1998). A syndrome produced by diverse nocuous agents. 1936. J. Neuropsychiatry Clin. Neurosci. 10, 230–231.
33. Vyas, A., Mitra, R., Shankaranarayana Rao, B.S., and Chattarji, S. (2002). Chronic stress induces contrasting patterns of dendritic remodeling in hippocampal and amygdaloid neurons. J. Neurosci. 22, 6810–6818.
34. King, L.R., McLaurin, R.L., Lewis, H.P., and Knowles, H.C., Jr. (1970). Plasma cortisol levels after head injury. Ann. Surg. 172, 975–984.
35. Bouzarth, W.F., Shenkin, H.A., and Feldman, W. (1968). Adrenocortical response to craniocerebral trauma. Surg. Gynecol. Obstet. 126, 995–1001.
36. Grundy, P.L., Harbuz, M.S., Jessop, D.S., Lightman, S.L., and Sharples, P.M. (2001). The hypothalamo-pituitary-adrenal axis response to experimental traumatic brain injury. J. Neurotrauma 18, 1373–1381.
37. Roe, S.Y., McGowan, E.M., and Rothwell, N.J. (1998). Evidence for the involvement of corticotrophin-releasing hormone in the pathogenesis of traumatic brain injury. Eur. J. Neurosci. 10, 553–559.
38. McDonald, A.J. (1992). Projection neurons of the basolateral amygdala: a correlative Golgi and retrograde tract tracing study. Brain Res. Bull. 28, 179–185.
39. Pitkanen, A., Pikkarainen, M., Nurminen, N., and Ylinen, A. (2000). Reciprocal connections between the amygdala and the hippocampal formation, perirhinal cortex, and postrhinal cortex in rat. A review. Ann. N. Y. Acad. Sci. 911, 369–391.
40. McDonald, A.J. (1992). Cell types and intrinsic connections of the amygdala, in: *The Amygdala: Neurobiological Aspects of Emotion, Memory, and Mental Dysfunction*. J.P. Aggleton (ed). Wiley-Liss: New York, pps. 67–96.
41. McDonald, A.J., Beitz, A.J., Larson, A.A., Kuriyama, R., Sellitto, C., and Madl, J.E. (1989). Co-localization of glutamate and tubulin in putative excitatory neurons of the hippocampus and amygdala: an immunohistochemical study using monoclonal antibodies. Neuroscience 30, 405–421.
42. Hausser, M., Spruston, N., and Stuart, G.J. (2000). Diversity and dynamics of dendritic signaling. Science 290, 739–744.
43. Lifshitz, J., Witgen, B.M., and Grady, M.S. (2007). Acute cognitive impairment after lateral fluid percussion brain injury recovers by 1 month: evaluation by conditioned fear response. Behav. Brain. Res. 177, 347–357.
44. Hallam, T.M., Floyd, C.L., Folkerts, M.M., Lee, L.L., Gong, Q.Z., Lyeth, B.G., Muizelaar, J.P., and Berman, R.F. (2004). Comparison of behavioral deficits and acute neuronal degeneration in rat lateral fluid percussion and weight-drop brain injury models. J. Neurotrauma 21, 521–539.
45. Ridet, J.L., Malhotra, S.K., Privat, A., and Gage, F.H. (1997). Reactive astrocytes: cellular and molecular cues to biological function. Trends Neurosci. 20, 570–577.
46. Elder, G.A., Dorr, N.P., De Gasperi, R., Gama Sosa, M.A., Shaughness, M.C., Maudlin-Jeronimo, E., Hall, A.A., McCarron, R.M., and Ahlers, S.T. (2012). Blast exposure induces post-traumatic stress disorder-related traits in a rat model of mild traumatic brain injury. J. Neurotrauma 29, 2564–2575.
47. Heldt, S.A., Elberger, A.J., Deng, Y., Guley, N.H., Del Mar, N., Rogers, J., Choi, G.W., Ferrell, J., Rex, T.S., Honig, M.G., and Reiner, A. (2014). A novel closed-head model of mild traumatic brain injury caused by primary overpressure blast to the cranium produces sustained emotional deficits in mice. Front. Neurol. 5, 2.
48. Kovesdi, E., Kamnaksh, A., Wingo, D., Ahmed, F., Grunberg, N.E., Long, J.B., Kasper, C.E., and Agoston, D.V. (2012). Acute minocycline treatment mitigates the symptoms of mild blast-induced traumatic brain injury. Front. Neurol. 3, 111.
49. Meyer, D.L., Davies, D.R., Barr, J.L., Manzerra, P., and Forster, G.L. (2012). Mild traumatic brain injury in the rat alters neuronal number in the limbic system and increases conditioned fear and anxiety-like behaviors. Exp. Neurol. 235, 574–587.
50. Herry, C., Ciocchi, S., Senn, V., Demmou, L., Muller, C., and Luthi, A. (2008). Switching on and off fear by distinct neuronal circuits. Nature 454, 600–606.
51. Jasnow, A.M., Ehrlich, D.E., Choi, D.C., Dabrowska, J., Bowers, M.E., McCullough, K.M., Rainnie, D.G., and Ressler, K.J. (2013). Thy1-expressing neurons in the basolateral amygdala may mediate fear inhibition. J. Neurosci. 33, 10396–10404.

Address correspondence to:
Theresa Currier Thomas, PhD
Department of Child Health
University of Arizona College of Medicine-Phoenix
425 North 5th Street
ABC-1 Building, Room 320
Phoenix, AZ 85004-2157

E-mail: theresathomas@email.arizona.edu